Three-Dimensional Reconstruction and Analysis of Mitotic Spindles from the Yeast, *Schizosaccharomyces pombe*

Rubai Ding, Kent L. McDonald, and J. Richard McIntosh

Laboratory for Three Dimensional Fine Structure, Department of Molecular, Cellular, and Developmental Biology, University of Colorado, Boulder, Colorado 80309-0347

Abstract. Mitotic spindles of *Schizosaccharomyces pombe* have been studied by EM, using serial cross sections to reconstruct 12 spindles from cells that were ultrarapidly frozen and fixed by freeze substitution. The resulting distributions of microtubules (MTs) have been analyzed by computer. Short spindles contain two kinds of MTs: continuous ones that run from pole to pole and MTs that originate at one pole and end in the body of the spindle. Among the latter there are three pairs of MT bundles that end on fibrous, darkly staining structures that we interpret as kinetochores. The number of MTs ending at each putative kinetochore ranges from two to four; all kinetochore-associated MTs disappear as the spindle elongates from 3–6 μm. At this and greater spindle lengths, there are no continuous MTs, only polar MTs that interdigitate at the spindle midzone, but the spindle continues to elongate. An analysis of the density of neighboring MTs at the midzone of long spindles shows that their most common spacing is ~40 nm, center to center, and that there is a preferred angular separation of 90°. Only hints of such square-packing are found at the midzone of short spindles, and near the poles there is no apparent order at any mitotic stage. Our data suggest that the kinetochore MTs (KMTs) do not interact directly with nonkinetochore MTs, but that interdigitating MTs from the two spindle poles do interact to form a mechanically stable bundle that connects the poles. As the spindle elongates, the number of MTs decreases while the mean length of the MTs that remain increases. We conclude that the chromosomes of *S. pombe* become attached to the spindle by kinetochore MTs, that these MTs disappear as the chromosomes segregate, that increased separation of daughter nuclei is accompanied by a sliding apart of anti-parallel MTs, and that the mitotic processes of *S. pombe* are much like those in other eukaryotic cells.

MITOSIS in yeast is currently receiving considerable attention from geneticists and molecular biologists (for examples see Carbon and Clark, 1990; Hoyt et al., 1990; Nurse, 1990; Winey et al., 1991; Yanagida, 1991), but structural work on these organisms has been comparatively limited, in part because of the difficulty of preserving the cells for EM. Yeasts are, however, attractive specimens for a cell biological analysis of mitosis, because they are small enough to permit detailed study (Byers, 1981), and because they have fewer microtubules (MTs)[1] and usually fewer chromosomes than higher eukaryotic cells. Further, many yeast cell cycle mutants are available, some with effects on mitosis, and one may hope that thorough ultrastructural analysis of phenotype in such strains will help to elucidate the mechanisms of chromosome motion.

We have chosen *Schizosaccharomyces pombe* for this study of spindle structure because several features of its cell biology are similar to those of higher eukaryotes. Its cell cycle includes a G2 phase (Mitchison, 1990), followed by a prophase when the centrosomes separate (Kanbe et al., 1990), and its three chromosomes condense for mitosis to become discrete objects, visible in the light microscope (Fischer et al., 1975; Robinow, 1977). Its spindle forms for the occasion of karyokinesis and disassembles as the process is completed (Hagan and Hyams, 1989). Its centromeres are complex structures that require tens of thousands of DNA bases for normal chromosome segregation (Clarke and Baum, 1990; Carbon and Clarke, 1990). The information available therefore suggests that *S. pombe* is likely to be a good model system for a rigorous study of mitosis.

The mitotic spindle of *S. pombe* was initially studied by McCully and Robinow (1971), using both light and electron microscopy. They interpreted their images to suggest that chromosomes were attached directly to the spindle pole bodies (SPBs), so they referred to the SPB as a "kinetochore equivalent." Tanaka and Kanbe (1986) used EM to study longitudinal sections of mitotic cells fixed by plunge freezing and freeze substitution. Based on images obtained with this superior method of preservation, they proposed that mitosis was accomplished by a shortening of chromosomal MTs, together with an elongating of the pole–pole MTs that com-

1. *Abbreviations used in this paper*: HPF, high pressure freezing; KMT, kinetochore MT; MT, microtubule; SPB, spindle pole bodies; 3D, three-dimensional.

prised the intranuclear spindle. The evidence for both these conflicting views was, however, limited by the lack of three-dimensional (3-D) information about the positions and trajectories of the relevant spindle MTs.

To understand the design of a particular spindle and to learn how it attaches to and moves chromosomes, it is useful to obtain complete information about the organization of its microtubules (McIntosh et al., 1975*a*) using the best fixation available. This task is most rigorously accomplished by using fast frozen, freeze-substituted material to minimize fixation artifacts (Nicolas, 1991) and by building models of the spindle based on cross sections that allow one to follow each MT from one of its ends to the other without ambiguity (McIntosh et al., 1975*b*; McDonald et al., 1977). This paper describes such results.

To aid in the 3-D reconstruction of spindles and to facilitate a more quantitative analysis of the resulting models, we have used a computer to help align images of successive sections and abstract MT coordinates from the images, then to build graphic models that represent MT trajectories, and to analyze the resulting structures in 3-D. Our results from this study suggest that mitosis in *S. pombe* is an "orthodox" eukaryotic cell division with a particularly well organized spindle that should be useful for cell biological as well as molecular analysis.

Materials and Methods

S. pombe, strain cdc25-22, was grown at the permissive temperature to mid-log phase in MY medium (Tanaka and Kanbe, 1986). The cells were then frozen by either of two methods: plunging into liquid ethane (Howard and Aist, 1979) or high pressure freezing (HPF) (Moor, 1987; Dahl and Staehelin, 1989). Following either freezing method, the cells were fixed and dehydrated by freeze substitution in acetone containing 2% OsO_4 and 0.05% uranyl acetate at −90°C for 2–4 d in a homemade freeze substitution device (Kiss and McDonald, 1993). Samples were allowed to warm slowly to −20°C and held at that temperature for about 3 h. They were then warmed to 0°C for 1.5 h and to room temperature for ~0.5 h. Fixed cells were then rinsed with acetone several times and gradually infiltrated and embedded in Epox-Araldite. Cells frozen by HPF showed preservation of a somewhat higher quality, and all of the micrographs in this paper were prepared with this method.

Serial sections 60 nm thick were cut with a Reichert Ultracut E (Reichert Jung, Vienna), picked up on formvar-coated slot grids, stained with 1% uranyl acetate and lead citrate, and imaged in JEOL-100C electron microscope (JEOL USA Inc., Peabody, MA) operating at 80 kV. Spindle length has been estimated from the number of serial cross sections required to go from one pole to the other. Since our microtome cuts sections of uniform thickness to an excellent approximation, the relative lengths of spindles are accurate to ~5%; their absolute lengths are probably accurate to about ~10%. Relative spindle length is important, because throughout this investigation we have used spindle length as a way to estimate relative stage in mitosis.

Serial cross sections through mitotic spindles were photographed at a magnification of ~16,000, and the relevant parts of these negatives were digitized with a Dage video camera (Dage-MTI, Inc., Wabash, MI) and a Parallax image processor, hosted in a MicroVax computer, as described in McDonald et al. (1991). Spindle MTs were tracked for the entire length of every spindle studied, and a 3-D model of these polymers was built in the computer. MT distributions were then analyzed by computer, using programs written by David Mastronarde of our lab, and described in McDonald et al. (1991; 1992).

Results

The Fine Structure of S. pombe After Cryofixation and Freeze Substitution

Our methods have produced images of *S. pombe* in which most features of cell fine structure are well preserved (Fig. 1). The wall that surrounds the cell is constructed in three layers: the outermost is filamentous with elements that project radially outward from an underlying layer that is less electron dense. The innermost layer of the wall is apposed to the plasma membrane and comprises a thin, electron-dense lamina. The cell membrane itself contains invaginations, suggesting that either endocytic and/or exocytic processes were occurring at the time of fixation. The cytoplasm is rich with ribosomes, but it also contains the other expected organelles: mitochondria with evident cristae, ER, vacuoles, a nucleus whose envelope contains nuclear pores, and some cytoplasmic vesicles of unknown function. Within the nucleus of this mitotic cell, the spindle can be seen in cross section, surrounded by darkly staining material, probably from the persistent nucleolus.

The Spindle Pole Body (Centrosome)

The spindle pole bodies (SPBs) of mitotic cells are composed of electron-dense materials assembled at the nuclear envelope. One SPB from an early mitotic stage (spindle length, 2.3 μm) is shown in Fig. 2, *A–F*, and one from a later mitotic stage (chromosomes already at the pole; spindle length, 8.0 μm) is shown in Fig. 3, *A–F*. The nuclear positions and orientations of these two sets of micrographs are marked on Figs. 2 *G* and 3 *G*, respectively. The SPB is located largely at the cytoplasmic surface of the nuclear membrane, but some images suggest that during mitosis it may penetrate into the nuclear membrane (see also McCully and Robinow, 1971; Heath, 1981; Tanaka and Kanbe, 1986). At both mitotic stages shown here, SPBs include a protrusion of darkly staining material that lies perpendicular to the spindle axis.

During early mitosis, a SPB marks one end of >20 spindle MTs (Fig. 2). By the middle of spindle elongation (spindle length, ~6 μm), the number of MTs at a SPB has decreased to about eight, and by a spindle length of 8 μm, the number is six (Fig. 3). This change is not accompanied by a decrease in the apparent area of the SPB. The arrow in Fig. 3 *C* identifies an MT that extends for only one or two sections. Such short MTs immediately associated with the poles are not found in short spindles but are common in longer ones. At this time there are also a few MTs that grow from the SPB and project into the cytoplasm (Fig. 3 *A*, *arrow*). In both Figs. 2 and 3 there is an electron-lucent matrix near the SPB but lying beneath the nuclear envelope and pervading the space around the spindle MTs (Figs. 2 *D* and 3, *C* and *D*). In all the spindles that we have observed, we found that all the MTs were associated with one SPB or the other, suggesting that spontaneous initiation of MTs in the nucleus of *S. pombe* is rare.

Kinetochores and Kinetochore MTs

Fig. 4 shows images from a set of serial sections cut near the midregion of a short mitotic spindle (2.3 μm). Fig. 4 *F* depicts the positions of Fig. 4, *A–E* along the spindle axis. Some of the MTs end on dark, fibrillar material (see brackets, Fig. 4, *B–D*). The top brackets in the series mark two such MTs and their associated dark structure, and the bottom set marks three that end in a similar way. Each short spindle contains three pairs of these structures; the members of each pair are aligned along the spindle axis, and in the

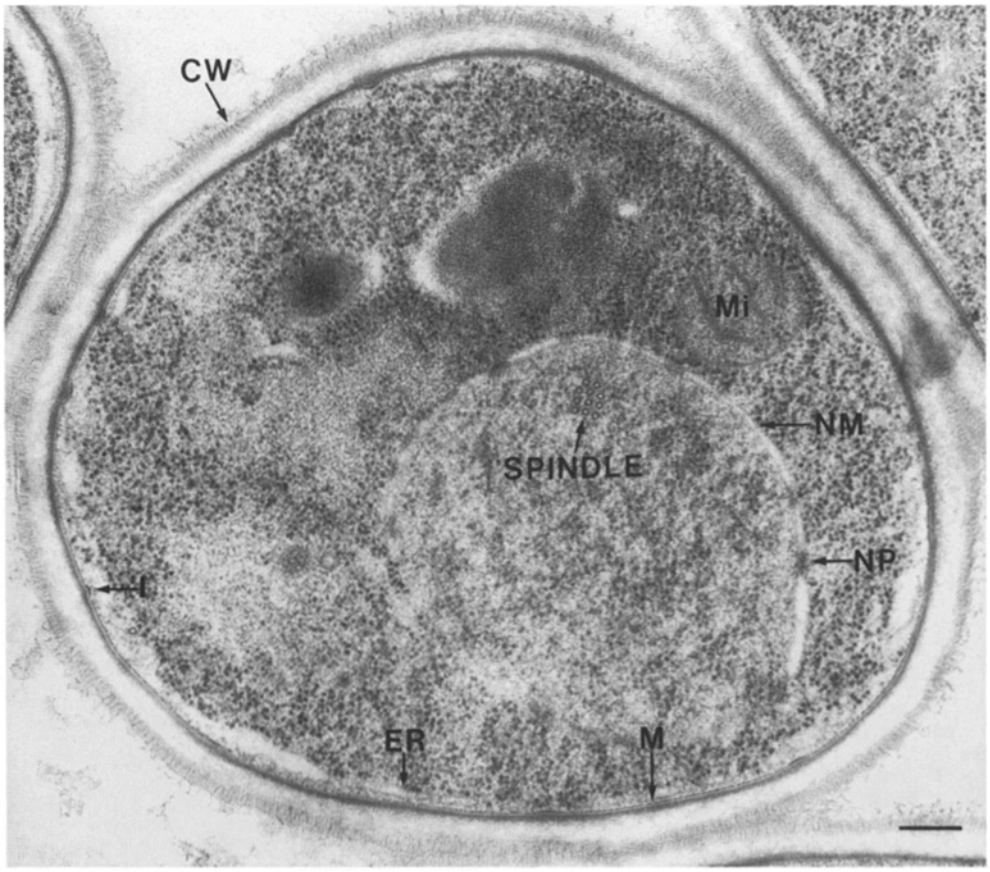

Figure 1. An electron micrograph of *S. pombe*, cut in cross section. The cell wall, the plasma membrane, cytoplasm, and the nucleus are all clear. A spindle is seen in cross section. *NP*, nuclear pore; *NM*, nuclear membrane; *M*, cell membrane; *CW*, cell wall; *Mi*, mitochondrion; *ER*, endoplasmic reticulum; and *I*, invagination. Bar, 0.2 μm.

shortest spindles the members of each pair are separated by only ~0.3 μm. We interpret these structures as kinetochores and will refer to them as such for the remainder of this paper. The number of MTs ending at each kinetochore varies from two to four with a mean value of three. The number of kinetochore MTs (KMTs) ending on sister kinetochores is not always the same; we have seen two MTs ending on one kinetochore and three on its sister, as well as three on one and four on its sister.

Three-Dimensional Reconstructions of Early Mitotic Spindles

The model shown in Fig. 5 *A* was constructed from serial sections through a spindle ~2.3 μm long, which we interpret as early in mitosis. It contains two categories of MTs: continuous ones that start at one SPB and end at the other (Fig. 5 *B*) and shorter MTs that originate from one pole and end before reaching the other (Fig. 5, *C* and *D*). The latter MTs include six clusters of KMTs, as defined above, and these together with the six contours that mark the boundaries of the dark-staining material are shown in Fig. 5 *E*. The dark-staining material is most evident one section beyond the ends of these MTs, which accounts for the gap between the two components of the computer-drawn model. The mean length of all the KMTs defined in this model is 0.78 $\pm$ 0.15 μm.

Fig. 6 shows a spindle that is ~2.8 μm long. Here the distances between each pair of oppositely oriented kinetochores range from 0.48 to 1.04 μm (Fig. 6 *C*); the mean separation is obviously greater than that seen in Fig. 5. The greater separation of what appear to be sister kinetochores is consistent with our interpretation that longer spindles are later in mitosis than shorter ones. The variation in the distance between pairs of sister kinetochores may mean either that the time at which chromosome separation begins is not synchronized for all chromosomes or that the speed of chromosome separation is not uniform. Note, however, that the mean length of the KMTs in this cell is 0.75 $\pm$ 0.28 μm, not significantly shorter than the mean KMT length seen in the shorter spindle. It appears that anaphase in *S. pombe* begins with spindle elongation. Another difference between these two spindle models is that there are four continuous MTs in the short spindle but only one in the longer.

Arrangements of Spindle MTs Near the Poles and at the Midzones of Spindles with Various Lengths

Fig. 7, *A* and *B* show the MTs in sections cut near the pole and at the midzone, respectively, of the mitotic cell shown in Fig. 5 *A* (arrows in the latter figure indicate the positions of these sections). There is no obvious organization in the MT arrangement at either position along the spindle. Near the pole (Fig. 7 *A*), the MTs are embedded in a dark-staining fibrillar matrix. In the midzone (Fig. 7 *B*), MTs are surrounded by a mixture of fibrillar and granular material which may represent chromatin and nucleolar remnant. The different kinds of MTs, as identified from the 3-D models, are indicated in Figs. 7, *A'* and *B'*. KMTs in Fig. 7 *A* lie near the periphery of the spindle, but no other order is evident. In Fig. 7 *B*, the one cluster of KMTs is seen near the periphery (Fig.

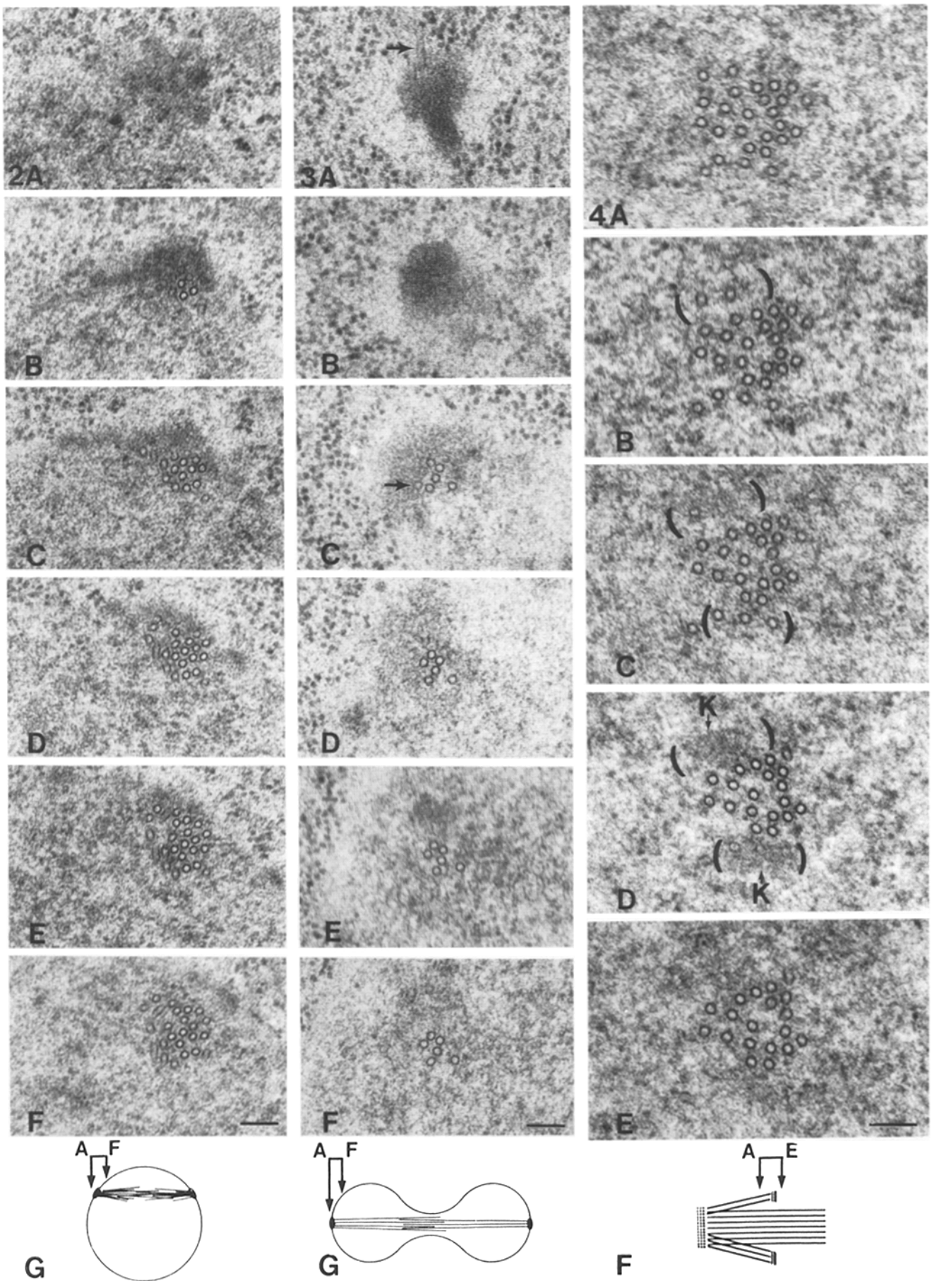
2A
3A
4A
B
B
B
C
C
C
D
D
D
K
K
E
E
E
F
F
F
A F
A F
A E
G
G
F

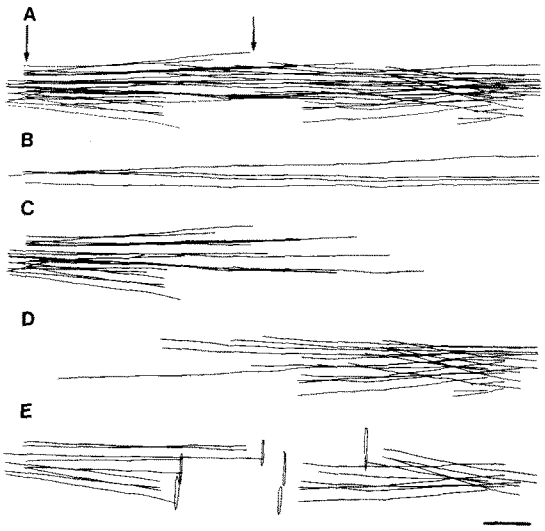

Figure 5. A set of models built from micrographs of a short mitotic spindle (2.3 μm) displayed in side view. *A* shows all the MTs of the spindle. The arrows identify the positions of the sections shown in Fig 7. *B* shows the MTs that run all the way from one pole to the other. *C* and *D* show the MTs that emanate from each pole. Among these MTs are KMTs, which are shown in *E*. The closed polygons in *E* mark the positions of dark-staining material that we interpret as kinetochores. The distances between sister kinetochores are ~300 nm. Bar, 0.2 μm.

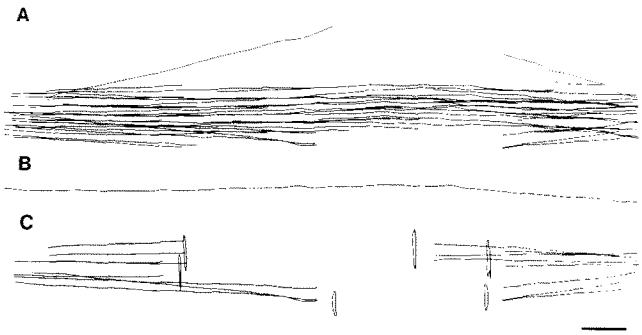

Figure 6. A set of models from an early mitotic spindle whose length is ~2.8 μm. *A* shows all the spindle MTs. *B* shows the only continuous MT, and *C* shows the KMTs and kinetochores. The distances between each pair of sister kinetochores vary from 0.8 to 1.04 μm. Bar, 0.2 μm.

7 *B'*), but again little order is apparent. Polarities cannot be assigned to the continuous MTs, so the possibility of any preferential associations between antiparallel MTs is difficult to assess at this stage of mitosis.

Fig. 8, *A–C* show models constructed from an 8-μm spindle. Note that the scaling of these models has been changed from that of Figs. 5 and 6 for convenience of display. By this stage, the chromosomes have already arrived at the poles, and KMTs are not evident. Other MTs, however, emanate from each pole and interdigitate at the spindle midzone (Fig. 8, *B* and *C*). This mitotic stage contains no continuous MTs. Fig. 9, *A* and *B* show the cross-sectional arrangements of MTs from the polar and midzone regions of the spindle shown in Fig. 8 *A* (*arrows* in Fig. 8 *A* show the positions of these two sections). No special MT arrangement is seen at the pole (Fig. 9 *A*), but there is a highly organized MT packing in the zone of interdigitation (Fig. 9 *B*). In Fig. 9 *B'*, the open and closed circles indicate the MTs from opposite poles. The square-packed arrangement of MTs is formed by alternating MTs from the two poles. Bridges between adjacent MTs in this configuration are sometimes seen (e.g., Fig. 9 *C*, *arrows*).

A Neighbor Density Analysis of MTs at the Pole and the Midzone

We have analyzed MT packing at several places in the spindle and at different times during mitosis, using algorithms described elsewhere (McDonald et al., 1991, 1992). Fig. 10, *A–D* show the results from such an analysis of the cell displayed in Fig. 5, and Fig. 11, *A–D* describe the cell shown in Fig. 8. Near the poles of short spindles (e.g., Fig. 7 *A*), there is a peak at ~35 nm in the radial density distribution and at ~60° in the distribution of angular spacings; these results suggest that the MTs near the poles of a short spindle are roughly close packed. We have looked for specific spacings or angles between KMTs and other spindle MTs, but found none. At the midzone of the same spindle, there is a broader peak in the radial density distribution and no well-defined peak in the distribution of angular frequencies (Fig. 10, *C* and *D*). These results confirm that there is little order in the cross sectional arrangements of MTs in the early spindle of *S. pombe*.

The MT arrangements near the poles of a longer mitotic spindle show no specific peak in either the distance analysis or angular analysis (Fig. 11, *A* and *B*). At the zone of interdigitation, on the other hand, when the MTs form a noticeably square-packing array (corresponding to Fig. 9 *B*), the distance analysis shows sharp peaks at ~40 nm and 2×40 nm with a smaller peak at $\sqrt{2} \times 40$ nm (Fig. 11 *C*), characteristic of a square packed array. The distribution of angular spacings peaks at 90° (Fig. 11 *D*), as expected.

These data and all results from other cells that have been analyzed in a similar way (data not shown) demonstrate that as the spindle elongates, the MTs at the midzone undergo a transition from a disorganized arrangement to a well-defined, square-packed array. For example, the MTs at the midzone of the spindle in Fig. 6, which is longer than the spindle in Fig. 5, appear more organized than in the earlier spindle, as is evident both from the micrographs and from the size of the peak in their radial density distributions, but square-packing as identified by the angular distribution, has not yet formed (data not shown). Our images suggest that the

Figures 2, 3, and 4. (Fig. 2) Serial sections from the region of the SPB in an early mitotic spindle. *G* depicts the positions of *A–F* in the nucleus and spindle. Bar, 0.1 μm. (Fig. 3) Serial sections from the region of the SPB in a late mitotic spindle. *G* depicts the positions of micrographs *A–F* in the nucleus and spindle. The arrow in *C* indicates an MT that runs for only one to two section(s). Bar, 0.1 μm. (Fig. 4) Serial sections from the region near the midzone of a short spindle. The brackets mark regions that we interpret as kinetochores and KMTs. *F* shows the positions of these micrographs in the spindle. *K*, kinetochore. Bar, 0.1 μm.

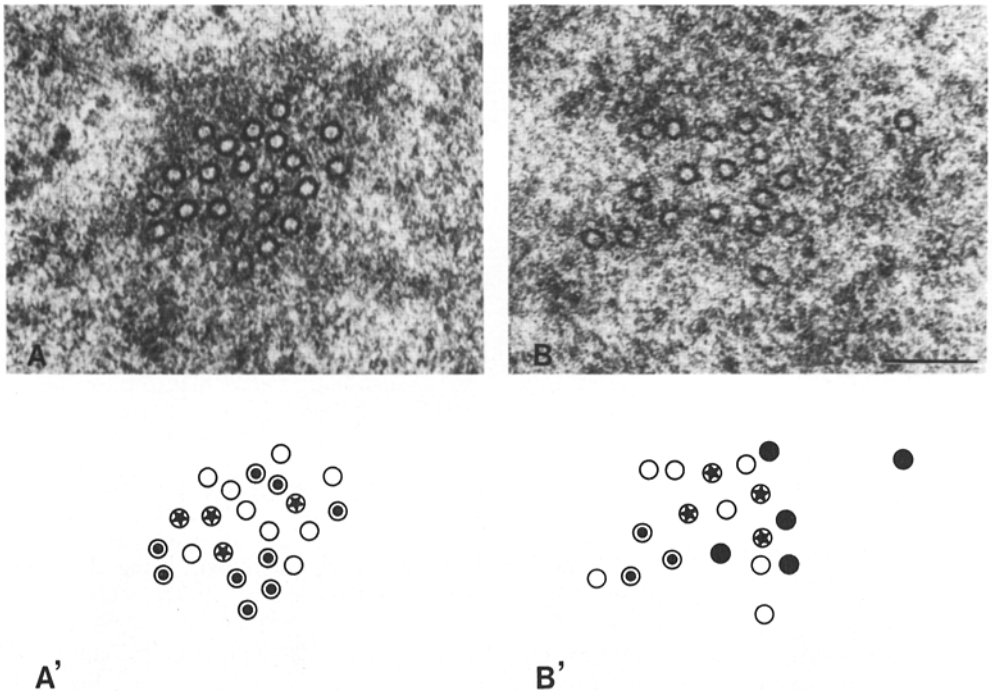

Figure 7. Cross-sectional views of MT arrangements in an early mitotic spindle. *A* shows the MTs near the pole and *B* the MTs at the midzone. The locations of these sections are indicated by the arrows in Fig. 5 *A*. *A'* and *B'* depict the identities of all the MTs in the cross sections, as determined from the 3-D models. (○) Noncontinuous MTs from one pole; (●) MTs from opposite pole; (◎) KMTs; and (✱) continuous MTs. Both micrographs show that MTs have no obviously organized pattern. Bar, 0.1 μm.

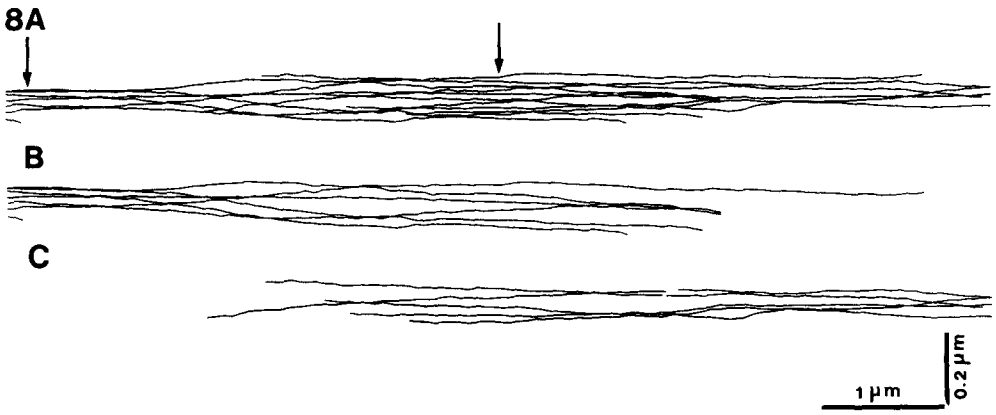

Figure 8. Models from a late mitotic spindle ~8 μm long. *A* shows the whole spindle, while *B* and *C* show the MTs associated with one pole or the other. The arrows indicate the positions of the sections shown in Fig. 9. By the time the spindle has reached this length, no continuous MTs remain. Bars: (x-axis) 1 μm; (y-axis) 0.2 μm.

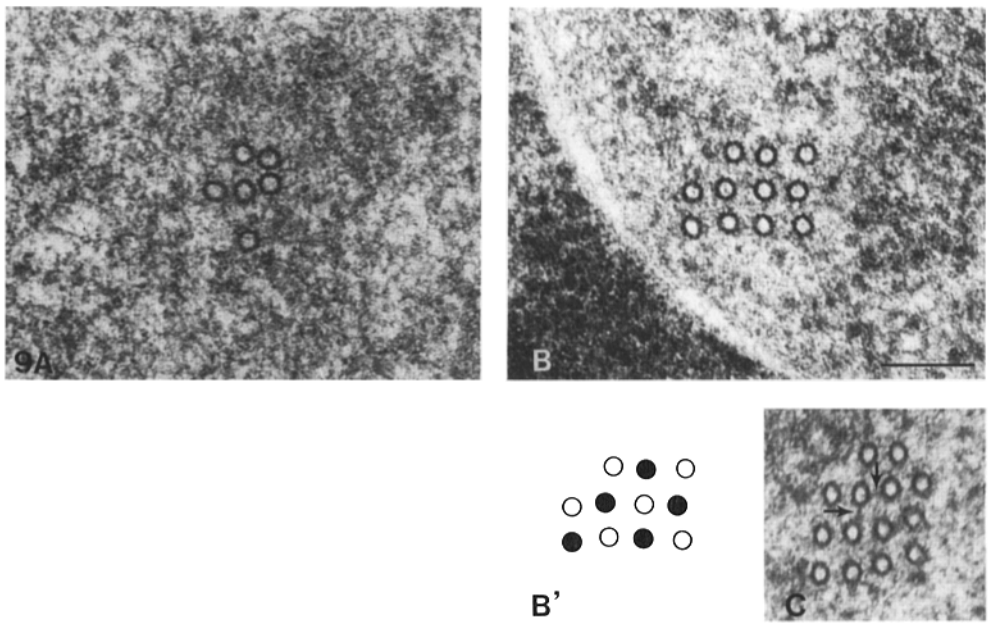

Figure 9. MT arrangements from a late mitotic spindle. *A* shows the MTs near the pole and *B* shows the square-packed MTs at the zone of overlap. The locations of these sections are indicated by the arrows in Fig. 8 *A*. The open circles and the filled ones represent MTs from opposite poles. The square-packed MTs alternate in their pole association, as shown in *B'*. The arrows in *C* indicate the bridges between the adjacent MTs. Bar, 0.1 μm.

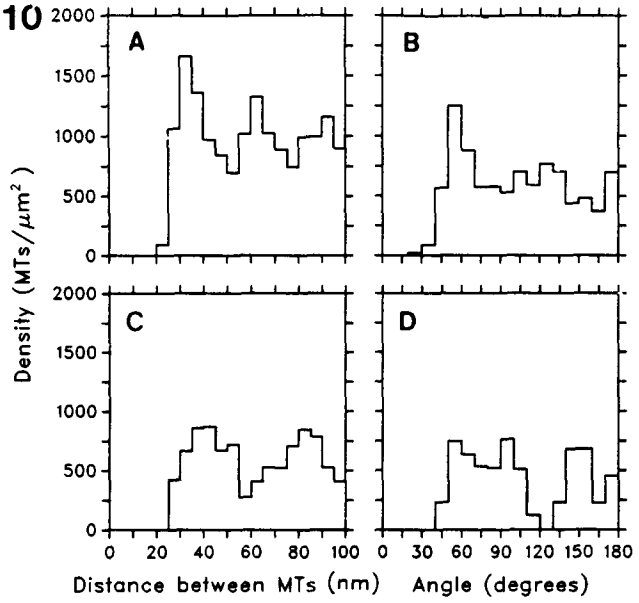

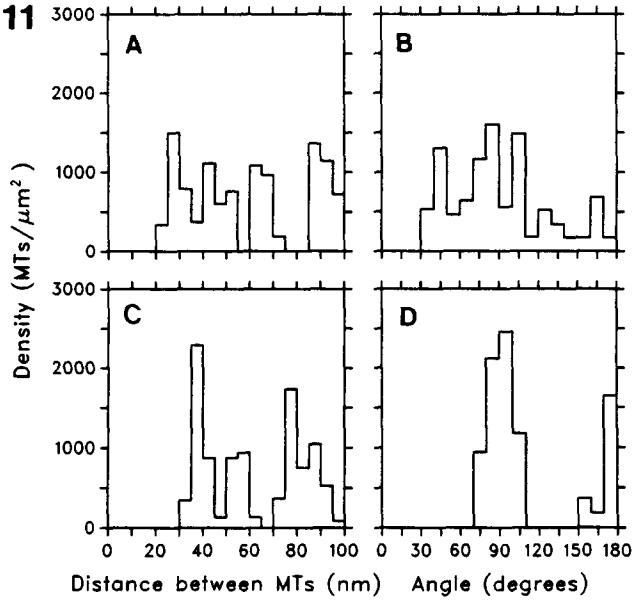

Figures 10 and 11. (Fig. 10) A neighbor density analysis for the MTs from a short mitotic spindle (the one shown in Fig. 5). *A* and *C* display the frequency with which MTs are found at a given spacing, while *B* and *D* show the distributions of the angular spacings between neighbors. *A* and *B* show data from MTs near the poles, while *C* and *D* describe MTs from the midzone. The MTs at the pole are clustered with a spacing of ~35 nm and an angular spacing of ~60°. There is a wide range of MT spacings at the spindle midzone and no clear peak in the angular distribution. (Fig. 11) Neighbor density analysis for MTs from a long mitotic spindle (the one shown in Figs. 8 and 9). *A–D* are as in Fig. 10. The region near the pole shows no clear peaks for both the neighbor density analysis (A) and angular analysis (B). The midzone shows a sharp peak at 40 nm (C) and at 90° (D).

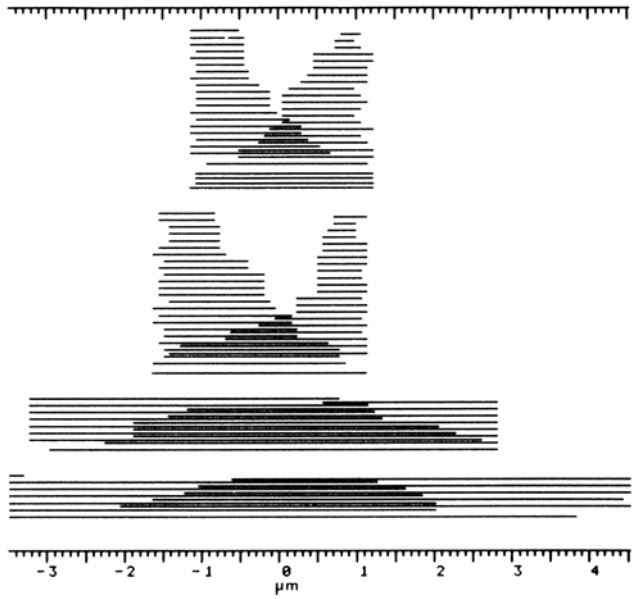

Figure 12. Four spindle models prepared from cells frozen by HPF. The MTs are presented as straight lines whose lengths and positions reflect the sections where each MT was found, and the lines in each model are arranged top to bottom in order of increasing length. The number of MTs decreases as the spindle elongates and the number of continuous MTs drops to zero.

emergence of spindle order is complete at about the time that the chromosomes arrive at the poles.

A Comparison of Spindle Design over a Wide Range of Lengths

Fig. 12 shows four pole–pole spindle reconstructions made from cells processed by HPF; the MTs have been projected as straight lines to permit easy comparison. All these cells were fixed in the same sample, so their states of preservation should be as similar as possible. The models have been aligned horizontally about the lines of symmetry in their pattern of MT interdigitation, and it is immediately evident that the spindles themselves are not perfectly symmetric. They have been arranged vertically in order of increasing spindle length to display a progression analogous to that which probably occurs over time in mitosis. From the shortest spindle to longest there is an increase in length from 2.3 to 8.0 μm. The continuous MTs decrease from 4 to 1 to 0 in going from the shortest spindle to the second shortest to the next, and all longer spindles contain no continuous MTs.

Fig. 13 shows seven models constructed from cells frozen by plunging into liquid ethane. These cells were grown at 28°C to minimize the cell wall thickness. Thick cell walls create problems during fixation and embedding. The cells and spindles in these preparations are longer than any found after HPF of cells grown at 25°C. Since *S. pombe* cells grown at 28°C are longer than those grown at 25°C, we suspect that this difference is a result of the difference in growth condition, not of freezing method. The design of the spindles in these cells is clearly similar to that seen after HPF, encouraging the view that both methods are preserving the normal arrangement of MTs.

These models again show a progression from short to long spindles with a loss in both short MTs and continuous MTs

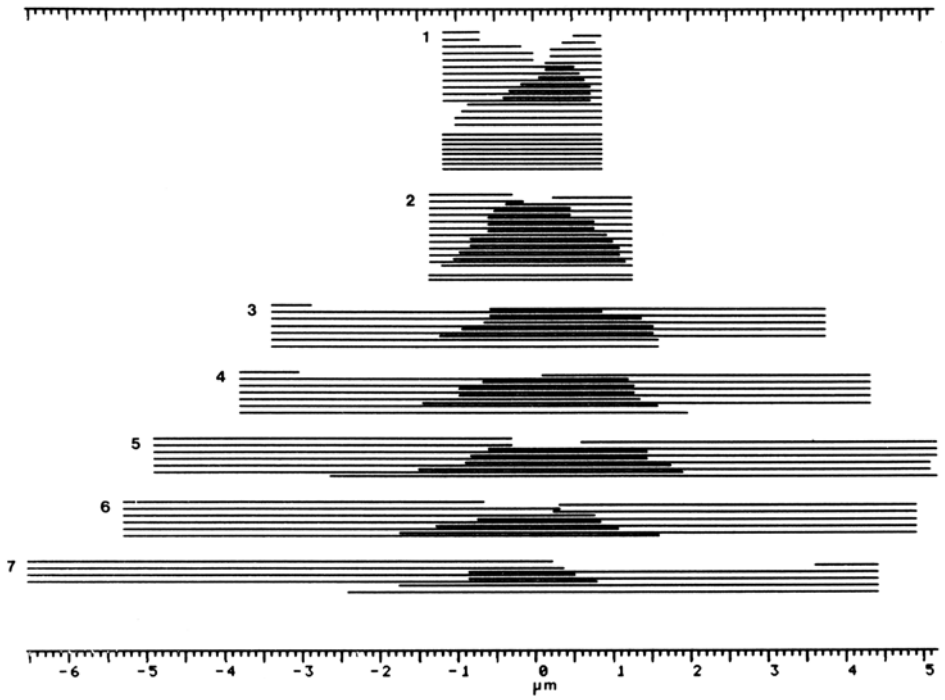

Figure 13. Seven spindle models prepared from cells frozen by plunge freezing. MT representations are as for Fig. 12. Note that there are some short MTs near the pole in spindles 3, 4, and 7.

as the spindle elongates. One of the short spindles preserved by plunge freezing showed evidence for kinetochores (data not shown). The more subtle differences between the models in Figs. 12 and 13, such as the greater number of MTs in the short spindles of the former than the latter, may be due simply to biological variation or the difference of growth condition. Note, however, that in spindles 3, 4, and 7 of Fig. 13 there is one MT in each that is too short to reach the zone of interdigitation; perhaps such MTs were fixed in the process of disassembling.

Fig. 14 shows the total length of MTs, the total length of MT overlap in the zone of interdigitation, and the total MT number for each of the models in Fig. 13. There is a small increase in total polymer while short spindles are elongating, but most of the increase in MT length that occurs during this time appears to be balanced by a decrease in the total MT number, suggesting that subunits released from MTs that are disappearing are recycled into the MTs that are elongating. At a spindle length of ~7 μm, the amount of total polymer begins to increase directly with spindle length, and during this time the number of MTs is constant. At a spindle length of ~10 μm, the amount of total polymer begins to decrease, and further spindle elongation is accompanied by a decrease in the extent of MT overlap. These results suggest that both MT polymerization and MT sliding contribute to spindle elongation in *S. pombe* and that the balance between these two processes changes during anaphase.

Some spindles twist about their long axis as they increase in length. This behavior is obvious in the stereo images shown in Fig. 15. The rotation is clear in many late spindles but is not detected in our images from early mitosis.

Discussion

We have used high pressure or plunge freezing and freeze-substitution fixation to preserve the structure of *S. pombe* for a detailed analysis of its mitotic spindle. Cryofixation improves morphological preservation, as shown by Tanaka and Kanbe (1986), but it also improves the time resolution of fixation. Cryofixation takes place in milliseconds (Gilkey and Staehelin, 1986) rather than the seconds or even minutes required for chemical crosslinking at room temperature (Hayat, 1989). This is important for a study such as ours because spindle MTs may show rapid shrinkage and growth (Saxton et al., 1984). The increase in fixation rate by several thousandfold is likely to be important for preserving MTs at their actual length for subsequent view in the electron microscope.

Our work extends published information by: (*a*) identifying the fine structure of kinetochores and enumerating the kinetochore MTs, (*b*) displaying the ordered packing of in-

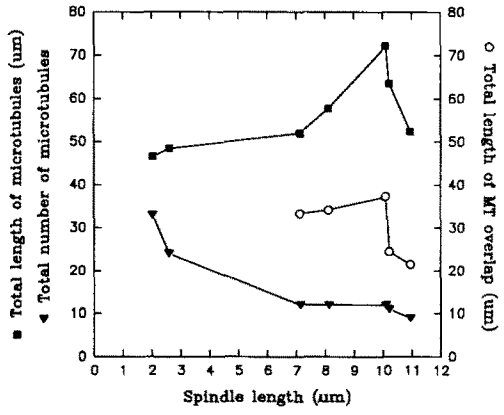

Figure 14. Total MT length (■), total overlap length (○) and total number of MTs (▲) plotted against spindle length for each spindle from Fig. 13. As the spindle elongates, the total length of MTs increases at first and then decreases. The length of MT overlap mimics this trend.

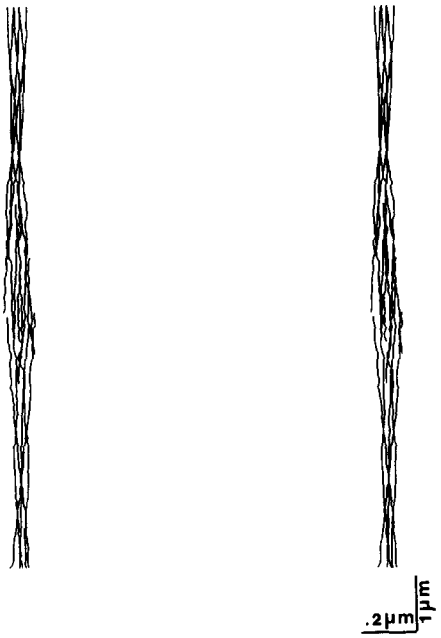

Figure 15. A stereo projection from a 3-D reconstruction of the spindle 6 shown as in Fig. 13. The MTs follow a helix around the axis of the spindle. Bars: (x-axis) 0.2 μm; (y-axis) 1.0 μm.

terdigitating MTs that emerges at the spindle midplane during mitosis, (*c*) giving us the length distribution of the spindle MTs at several stages during mitosis, and (*d*) revealing new aspects of spindle pole body structure and its relationship to spindle MTs.

Kinetochores and Kinetochore MTs

We have interpreted specific nuclear structures as kinetochores. This attribution has been based upon their location in early mitotic cells (near the spindle equator), their number (three pairs in early mitotic spindles, just the number of chromosomes in this organism), their staining density (they look similar to the kinetochores found in higher eukaryotes), their position relative to the ends of some spindle MTs (they are at the pole–distal ends of 2–4 MTs), and the fact that they separate as mitosis progresses. Additional evidence for the validity of this interpretation comes from the recent work of Uzawa and Yanagida (1992), who have used fluorescence in situ hybridization with a probe for centromeric DNA, to visualize centromeres in the light microscope. A structure recognized by their probe becomes double before mitosis, takes up a position near the middle of the spindle in early mitosis, and then separates from the middle to the two ends of the spindle as mitosis proceeds. The temporal and spatial redistribution of the structures we interpret as kinetochores correspond well to the material stained by Uzawa and Yanagida (1992).

The kinetochores in early mitotic cells of *S. pombe* are associated with the ends of 2–4 MTs, not the one MT that has been seen for *S. cerevisiae* (Peterson and Ris, 1976; King et al., 1982*a*), other fungi (Aist and Williams, 1972; Heath, 1974), slime molds (Roos, 1975), and *Dictyostelium discoideum* (Moens, 1976; McIntosh et al., 1985). Our results suggest, however, that there is a decrease in the number of KMTs as mitosis progresses. The total number of KMTs decreases from 19 in the cell shown in Fig. 5 to 16 in the cell shown in Fig. 6 and to ~0 in later stages of mitosis. We sometimes see MTs that are only a few sections long near the pole of a long spindle (e.g., the short MT seen in Fig. 3 *C*). These may be remnants of KMTs. Our observations suggest that KMTs in *S. pombe* shorten and decrease in number as the chromosomes segregate, as would be expected for anaphase A. The fact that the mean KMT length is no different between two spindles that are 2.3 and 2.8 μm long suggests, however, that anaphase A is not a distinct phase of mitosis that precedes anaphase B.

Our visualization of chromosomes in *S. pombe* is far from complete. We do find fibrous material of an unusual texture at the place where the chromosomes should be, according to both light microscopy and the location of the kinetochores. It is clear, however, that more reliable methods, like antibody staining, should be used to locate the chromosomes in the nucleus and to characterize their condensation during mitosis.

Structure of the Interpolar MT Bundle

The square packing of MTs in the zone of interdigitation during anaphase and telophase has not previously been reported for *S. pombe*. Similar packing has, however, been seen in prophase or prometaphase spindles of several diatoms (Tippit et al., 1975, 1978; McDonald et al., 1979), but anaphase MT packing in diatoms is generally hexagonal. In *D. discoideum*, on the other hand, the spindle is poorly organized during early mitosis and adopts a square packing arrangement in anaphase (McIntosh et al., 1985), just like the patterns seen here. Since no ordered arrangement is found at the spindle poles of either organism, it seems likely that the square-packing is a result of interactions between the interdigitating MTs from the two half spindles. The transition from a disordered packing at the midzone during early mitosis to the square-packing found in late spindles is consistent with the idea that the ordered geometry plays a role in late mitotic events, such as holding the two halves of a slender spindle together.

The elongation of spindles isolated from nuc2$^-$ cells of *S. pombe* after addition of ATP and tubulin suggests that a mechanochemical system in the zone of MT interdigitation cooperates with tubulin polymerization at the pole–distal MT ends to drive spindle elongation (Masuda et al., 1990). Such interactions may be mediated by mechanochemically important enzymes, such as kinesin-like proteins. The product of the *cut7* gene in *S. pombe* has been identified as kinesin-like on the basis of its predicted amino acid sequence (Hagan and Yanagida, 1990), and an antigen that is recognized by antibodies to CUT7 protein synthesized in bacteria binds to the zone of MT interdigitation (Hagan and Yanagida, 1992). This motor or one like it may therefore be one of the polypeptides that comprises the bridges we have seen between antiparallel MTs in the zone of overlap. As we have noted previously (McDonald et al., 1979; McIntosh et al., 1985), square packing requires that some energy, such as a specific MT cross-bridge, be put into the system to resist the natural tendency of packed fibers to assume a hexagonal pattern. The exact alternation of MTs from opposite poles along the square lattice is further evidence for specific interactions between adjacent antiparallel MTs.

Astral MTs arise in the cytoplasm of *S. pombe* during anaphase and telophase (Hagan and Hyams, 1988, and our

results). The role these fibers play in mitosis is still a matter of conjecture. Aist and co-workers (Aist and Berns, 1981; Aist and Bayles, 1991) have suggested that fungal nuclei are pulled apart late in anaphase by astral MTs, but the orientation of the cytoplasmic, SPB-associated MTs in *S. pombe* is oblique to the pole–pole axis (Hagan and Hyams, 1988, and our results) making it seem unlikely that such a system is important in this organism. Studies that inactivate one-motor system or another will be required to discriminate clearly between a "front wheel drive" and a mechanism for spindle elongation based on the interpolar MTs.

The observation that the spindle of *S. pombe* twists about its long axis during anaphase suggests that there are additional forces acting in or on the spindle during anaphase and telophase. We suggest that this may arise from a helical cant of the protofilaments in spindle MTs and the bunching together of the interdigitating MTs that becomes so marked in late anaphase. These interactions may throw the spindle MTs into a super coil to allow maximum interaction between neighbors.

Distributions of MT Length

Some of the MTs in short spindles are long enough to extend from one SPB to the other. The number of such MTs decreases as mitosis progresses, and by the middle of spindle elongation, this class of MTs has disappeared entirely. Clearly a *S. pombe* spindle can elongate without the benefit of continuous MTs. We suggest that the gradual disappearance of continuous MTs is caused by the conversion of continuous MTs into interdigitating MTs as the spindle elongates. The continuous MTs of early mitosis may play a scaffold function at the time when the chromosomes are separating, but we think it more likely that the continuous MTs are simply those interdigitating MTs that are long enough to reach the opposite pole, where their further growth is inhibited by the interaction of their plus ends with the SPB. Because of this apparent constraint on plus-end growth, the asymmetric nature of the SPB, and the fact that MTs at later stages may be stabilized by antiparallel interactions, it is not surprising that the MT length distributions in *S. pombe* do not conform to those predicted by dynamic instability (Kirchner and Mitchison, 1986).

The reduced number of MTs seen in long spindles of *S. pombe* suggests that some spindle MTs are losing their stability during anaphase, dissolving, and not being replaced. A decrease in MT number during mitosis has previously been described in several organisms, e.g., cultured mammalian cells (McIntosh and Landis, 1971), diatoms (McIntosh et al., 1979), and *S. cerevisiae* (King et al., 1982*a*,*b*) and this change may be a characteristic of mitosis. It seems likely that the MTs which depolymerize are the short MTs seen during anaphase (Fig. 13, spindles 3, 4, and 7). We suppose that MTs that lose their connections with other MTs in the zone of interdigitation, as the antiparallel MTs are sliding apart, become destabilized and depolymerize, allowing their subunits to recycle into the remaining MTs, promoting their further elongation (McIntosh et al., 1985). The small increase in total MT length during early anaphase is consistent with the idea that the subunits from depolymerized MT are recycled into the remaining polymers. Subsequent spindle MT behavior suggests, however, that the cell modulates tubulin dynamics during mitosis. When the spindle is ~7 μm, the amount of total polymer begins to rise and at ~11 μm, it begins to drop. The latter change occurs at the same time that the extent of MT overlap begins to decrease; it seems likely that a decrease in the rate of tubulin assembly relative to the speed of MT sliding promotes the decrease in MT overlap.

Peterson and Ris (1976) and King et al. (1982*b*) described continuous MTs in the spindles of *S. cerevisiae*. Both groups found that the number of continuous MTs decreased during mitosis, but even in very late anaphase, when only a single MT remained, it was interpreted as continuous. Our results are clearly different, since the continuous class of MTs is gone by mid anaphase. Further work will be required to determine whether this is a case of differences between yeasts or of differences in the methods used.

The Spindle Pole Body

The ultrastructure of the SPB in *S. pombe* has been previously described with sections cut perpendicular to the nuclear envelope (McCully and Robinow, 1971; Tanaka and Kanbe, 1986). Our results add to these descriptions by providing a view nearly parallel to the nuclear envelope as seen in Figs. 2 and 3. From this perspective, we see that the SPB occupies a roughly circular area, ~300–380 nm in diameter. The exact position of its outer boundary is difficult to determine in this view, because the outer margins of the SPB appear as an electron lucent area. This region may correspond to the "cytoplasmic zone of exclusion" typical of other Ascomycota and Basidiomycota (Heath, 1981). The functional significance of this zone is not yet known. We also see an osmiophilic projection from the SPB in the plane of the nuclear envelope. This may represent a structure associated with SPB duplication, such as the "bridge" seen in *S. cerevisiae* (Winey et al., 1991), but more detailed studies will be required to examine this possibility.

The relationship of the pole proximal MT ends to the SPB can readily be visualized in serial sections, such as those in Figs. 2 and 3 or by comparing Fig. 7, *A* and *A'* with Fig. 9 *A*. From these illustrations, and others not shown, it is evident that MTs in the region of the SPB are always tightly bunched, regardless of the phase of mitosis. This may mean that the pole proximal MT ends are not permanently attached to a particular region of the SPB, but are free to move around as other MTs are lost from the pole. Similar observations of "fluid" spindle poles have been made in diatoms (McDonald et al., 1979). Bridges occasionally seen between MTs may partly account for the clustering.

The activity of SPBs in *S. pombe* is also dynamic. Masuda et al. (1992) have shown that nucleation of spindle MTs from the SPB is regulated by cdc2 kinase. After metaphase, when cdc2 kinase becomes inactivated, SPBs are no longer capable of nucleating spindle MTs. Our observation that the number of spindle MTs decreases as anaphase begins, even though MT polymerization continues on existing MTs, is consistent with this finding. Interestingly, at this same time, MTs appear on the cytoplasmic side of the SPB (Hagan and Hyams, 1989; Tanaka and Kanbe, 1986) (Fig. 3 *A*). Whether these cytoplasmic MTs are nucleated or captured (Masuda et al., 1992) remains to be determined, but it is clear that further EM analysis of this interesting organelle will be important for understanding mitosis in *S. pombe*.

Conclusions

Our results suggest that mitosis in *S. pombe* includes chromosome attachment to KMTs, followed by motions that appear to correspond to anaphases A and B. These motions are based on both MT polymerization and MT sliding. We conclude that mitosis in *S. pombe* is generally similar to mitosis in other eukaryotes, and that this yeast is an attractive model for detailed study of chromosome motion.

We would like to thank Paul Nurse for the strain of *S. pombe* used, David Mastronarde for the development and application of 3-D reconstruction programs, Eileen O'Toole for help learning the computer analysis, Mary Morphew for help with the HPF and Dr. L. A. Staehelin for the generous use of his high pressure freezer.

This work was supported by National Institutes of Health grants RR00592 and GM 33787 to J. R. McIntosh.

Received for publication 7 August 1992 and in revsied form 21 September 1992.

References

Aist, J. R., and P. H. Williams. 1972. Ultrastructure and time course of mitosis in the fungus *Fusarium oxysporum*. *J. Cell Biol.* 55:368–389.

Byers, B. 1981. Cytology of the yeast cell cycle. *In* The Molecular Biology of the Yeast *Saccharomyces*: Life Cycle and Inheritance. J. N. Strathern, E. W. Jones, and J. R. Broach, editors. Cold Spring Harbor Laboratory, Cold Spring Harbor, NY. 59–96.

Carbon J., and L. Clarke. 1990. Centromere structure and function in budding and fission yeasts. *New Biol.* 2:10–19.

Clarke L., and M. P. Baum. 1990. Functional analysis of a centromere from fission yeast: a role for centromere-specific repeated DNA sequences. *Mol. Cell. Biol.* 10:1863–1872.

Dahl, R., and L. A. Staehelin. 1989. High pressure freezing for the preservation of biological structure: theory and practice. *J. Electron Microsc. Tech.* 3:165–174.

Fischer, P., M. Binder, and U. Wintersberger. 1975. A study of the chromosomes of the yeast *Schizosaccharomyces pombe* by light and electron microscopy. *Exp. Cell Res.* 96:15–22.

Gilkey, J. C., and L. A. Staehelin. 1986. Advances in ultrarapid freezing for the preservation of cellular ultrastructure. *J. Electron Microsc. Tech.* 3:177–210.

Hagan, I. M., and J. S. Hyams. 1989. The use of cell division cycle mutants to investigate the control of microtubule distribution in the fission yeast *Schizosaccharomyces pombe*. *J. Cell Sci.* 89:343–357.

Hagan, I., and M. Yanagida. 1990. Novel potential mitotic motor protein encoded by the fission yeast cut7+ gene. *Nature (Lond.).* 347:563–566.

Hagan, I., and M. Yanagida. 1992. Kinesin-related cut7 protein associates with mitotic and meiotic spindles in fission yeast. *Nature (Lond.).* 356:74–76.

Hayat, M. A. 1989. Principles and Techniques of Electron Microscopy. Third Edition. CRC Press, Boca Raton, FL. 469 pp.

Hayles, J., and P. Nurse. 1989. A review of mitosis in the fission yeast *Schizosaccharomyces pombe*. *Exp. Cell Res.* 184:273–286.

Heath, I. B. 1974. Mitosis in the fungus *Thraustotheca clavata*. *J. Cell Biol.* 60:204–220.

Heath, I. B. 1981. Nucleus-associated organelles in fungi. *Int. Rev. Cytol.* 69: 191–221.

Howard, R. J., and J. R. Aist. 1979. Hyphal tip ultrastructure of the fungus *Fusarium*: improved preservation by freeze substitution. *J. Ultrastruct. Res.* 66:224–234.

Hoyt, M. A., T. Stearns, and D. Botstein. 1990. Chromosome instability mutants of *Saccharomyces cerevisiae* that are defective in microtubule-mediated processes. *Mol. Cell. Biol.* 10:223–234.

Kanbe, T., Y. Hiraoka, K. Tanaka, and M. Yanagida. 1990. The transition of cells of the fission yeast b-tubulin mutant nda3-311 as seen by freeze-substitution electron microscopy: requirement of functional tubulin for spindle pole body duplication. *J. Cell Sci.* 96:275–282.

King, S. M., J. S. Hyams, and A. Luba. 1982*a*. Ultrastructure of mitotic spindles isolated from a cell division cycle mutant of the yeast, *Saccharomyces cerevisiae*. *Eur. J. Cell Biol.* 28:98–102.

King, S. M., J. S. Hyams, and A. Luba. 1982*b*. Absence of microtubule sliding and an analysis of spindle formation and elongation in isolated mitotic spindles from the yeast *Saccharomyces cerevisiae*. *J. Cell Biol.* 94:341–349.

Kirschner, M., and T. Mitchison. 1986. Beyond self-assembly: from microtubules to morphogenesis. *Cell.* 45:329–342.

Kiss, J. Z., and K. McDonald. 1993. EM immunocytochemistry following cryofixation and freeze substitution. *In* Methods in Cell Biology, Vol. 37, "Antibodies in Cell Biology." David Asai, editor. Academic Press, New York. In press.

Masuda, H., T. Hirano, M. Yanagida, and W. Z. Cande. 1990. In vitro reactivation of spindle elongation in fission yeast nuc2 mutant cells. *J. Cell Biol.* 110:417–425.

Masuda, H., M. Sevic, and W. Z. Cande. 1992. In vitro microtubule-nucleating activity of spindle pole bodies in fission yeast *Schizosaccharomyces pombe*: cell cycle-dependent activation in *Xenopus* cell-free extracts. *J. Cell Biol.* 117:1055–1066.

McCully, E. K., and C. F. Robinow. 1971. Mitosis in the fission yeast *Schizosaccharomyces pombe*: a comparative study with light and electron microscopy. *J. Cell Sci.* 9:475–507.

McDonald, K., J. D. Pickett-Heaps, J. R. McIntosh, and D. H. Tippit. 1977. On the mechanism of anaphase spindle elongation in *Diatoma vulgare*. *J. Cell Biol.* 74:377–388.

McDonald, K. L., M. K. Edwards, and J. R. McIntosh. 1979. Cross-sectional structure of the central mitotic spindle of *Diatoma vulgare*. *J. Cell Biol.* 83:443–461.

McDonald, K. L., D. Mastronarde, E. O'Toole, R. Ding, and J. R. McIntosh. 1991. Computer-based tools for morphometric analysis of mitotic spindles and other microtubule systems. *EMSA Bulletin.* 21:47–53.

McDonald, K. L., E. T. O'Toole, D. N. Mastronarde, and J. R. McIntosh. 1992. Kinetochore microtubules in PtK cells. *J. Cell Biol.* 118:369–383.

McIntosh, J. R., and S. C. Landis. 1971. The distribution of spindle microtubules during mitosis in cultured human cells. *J. Cell Biol.* 49:468–497.

McIntosh, J. R., W. Z. Cande, and J. A. Synder. 1975*a*. Structure and physiology of the mammalian mitotic spindle. *In* Molecules and Cell Movement. S. Inoue and R. E. Stephens, editors. Raven Press, New York. 31–76.

McIntosh, J. R., Z. Cande, J. Snyder, and K. Vanderslice. 1975*b*. Studies on the mechanism of mitosis. *Ann. NY. Acad. Sci.* 253:407–427.

McIntosh, J. R., K. L. McDonald, M. K. Edwards, and B. M. Ross. 1979. Three-dimensional structure of the central mitotic spindle of *Diatoma vulgare*. *J. Cell Biol.* 83:428–442.

McIntosh, J. R., U.-P. Roos, B. Neighbors, and K. L. McDonald. 1985. Architecture of the microtubule component of mitotic spindles from *Dictyostelium discoideum*. *J. Cell Sci.* 75:93–129.

Mitchison, J. M. 1990. The fission yeast, *Schizosaccharomyces pombe*. *BioEssays.* 12(4):189–191.

Moens, P. B. 1976. Spindle and kinetochore morphology of *Dictyostelium discoideum*. *J. Cell Biol.* 68:113–122.

Moor, H. 1987. Theory and practice of high pressure freezing. *In* Cryotechniques in Biological Electron Microscopy. R. A. Steinbrecht and K. Zierold, editors. Springer-Verlag, Berlin, Germany. 175–191.

Nicolas, G. 1991. Advantages of fast-freeze fixation followed by freeze-substitution for the preservation of cell integrity. *J. Electron Microsc. Tech.* 18:395–405.

Nurse, P. 1990. Universal control mechanism regulating onset of M-phase. *Nature (Lond.).* 344:503–508.

Peterson, J. B., and H. Ris. 1976. Electron-microscopic study of the spindle and chromosome movement in the yeast *Saccharomyces cerevisiae*. *J. Cell Sci.* 22:219–242.

Robinow, C. F. 1977. The number of chromosomes in *Schizosaccharomyces pombe*: light microscopy of stained preparations. *Genetics.* 87:491–497.

Roos, U.-P. 1975. Mitosis in the cellular slime mold *Polysphondylium violaceum*. *J. Cell Biol.* 64:480–491.

Saxton, W. M., D. L. Stemple, R. J. Leslie, E. D. Salmon, and J. R. McIntosh. 1984. Tubulin dynamics in cultured mammalian cells. *J. Cell Biol.* 99: 2175–2186.

Tanaka, K., and T. Kanbe. 1986. Mitosis in the fission yeast *Schizosaccharomyces pombe* as revealed by freeze-substitution electron microscopy. *J. Cell Sci.* 80:253–268.

Tippit, D. H., K. L. McDonald, and J. D. Pickett-Heaps. 1975. Mitosis in the centric diatom *Melosira varians*. *Cytobiologie.* 12:52–73.

Tippit, D. H., D. Schulz, and J. D. Pickett-Heaps. 1978. Analysis of the distribution of spindle microtubules in the diatom *Fragilaria*. *J. Cell Biol.* 79: 737–763

Uzawa, S., and M. Yanagida. 1992. Visualization of centromeric and nucleolar DNA in fission yeast by fluorescence *in situ* hybridization. *J. Cell Sci.* 101:267–275.

Winey, M., L. Goetsch, P. Baum, and B. Byers. 1991. MPS1 and MPS2: novel yeast genes defining distinct steps of spindle pole body duplication. *J. Cell Biol.* 114:745–754.

Yanagida, M. 1991. Control of mitotic chromosome disjunction in fission yeast. *In* Control of Cell Growth and Division. A. Ishihama and H. Yoshikawa, editors. Japan Sci. Soc. Press, Tokyo/Springer-Verlag, Berlin. 77–96.